Performance Characterisation of an Optical Fibre for ALPHA

Sarah Price
Durham University, Durham, UK

Abstract
Optical fibres present a simple, time-saving replacement to the use of a periscope for sending light over a large distance. This is a requirement for laser cooling of beryllium ions which sympathetically cool positrons in ALPHA, an important step in the production of trappable antihydrogen. The transmission losses of an LMA-10-PM fibre and its ability to correct the beam profile are presented here. A maximum transmission of (32.1 ± 0.3)% was found, however it is believed that this value could be improved with stretching of the fibre. It was also found that increasing the diameter of bends in the excess length of fibre improved the transmission up to a diameter of 38 cm, above which the transmission appeared to decrease again. It was shown that defects in the beam profile before entering the fibre were corrected when the fibre output was measured. Temperature effects were also investigated and it was found that an increase of 4.4 °C approximately halved the transmission from the fibre. In future, if the environment temperature continues to be unstable, a non-polarisation-maintaining fibre would be a more suitable choice.

Keywords
Optical fibre, ALPHA, bending losses, attenuation

1 Introduction

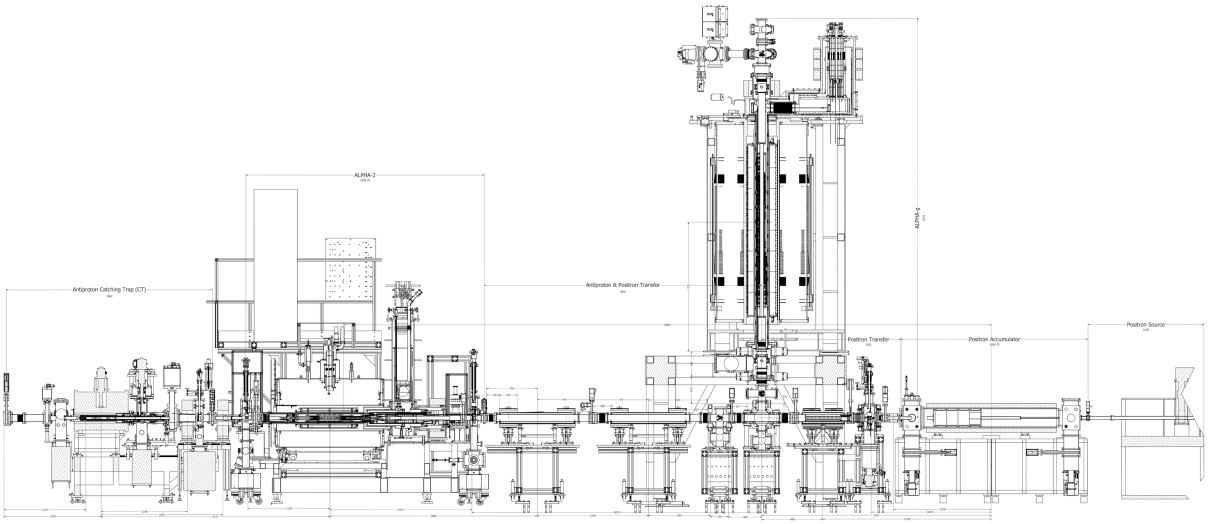

Figure 1: ALPHA apparatus [1].

Through production and trapping of antihydrogen atoms, the ALPHA experiment at CERN investigates the fundamental question: why is there more matter than anti-matter in our universe? Precision measurements of the properties of antihydrogen allow comparison with hydrogen, and symmetries between these atoms are explored.

The setup to produce antihydrogen is shown in Fig. 1. First, antiprotons from CERN's antiproton decelerator (AD) are captured in a high voltage Penning-Malmberg trap, known as the catching trap. Here they are sympathetically cooled with electrons, a technique in which the cold, low kinetic energy electrons undergo Coulomb interactions with the antiprotons, exchanging energy and lowering the kinetic energy of the antiprotons [2]. The plasma of antiprotons and electrons is also compressed using the strong drive rotating wall technique [3]. The antiprotons are then ejected to the recatching trap where this process is repeated. Simultaneously to the antiproton preparation, positrons are produced from a ^{22}Na source in a positron accumulator. The positron plasma is also compressed and cooled [2]. Mixing of positrons and antiprotons occurs in the atom trap. The plasmas are kept in potential wells which are slowly merged to allow the positrons and antiprotons to mix and produce antihydrogen atoms. The antihydrogen atoms are neutral but have a small magnetic dipole moment, allowing them to be trapped using magnetic fields. Without de-energising the magnetic trap the whole process can be repeated multiple times, known as stacking, and many antihydrogen atoms can be trapped at once [4]. If this process is completed in ALPHA-2, measurements of the internal structure of antihydrogen can be taken by shining lasers or microwaves onto the atoms. This same process can be done in ALPHA-g, with the apparatus oriented vertically instead. This allows measurement of the effect of gravity on antihydrogen.

To be able to trap antihydrogen it must be cold, approximately 0.5 K. It has been shown that during mixing the antiprotons thermally equilibrate with the positrons, so the temperature of the positrons defines the temperature of the antihydrogen [5]. Therefore, laser-cooled beryllium ions (Be+) have been introduced to ALPHA-2 to sympathetically cool the positrons before mixing. A 355 nm laser produces the Be+ ions by ablation of Be metal, and a 313 nm laser is used to cool the Be+ ions [6].

The current method for directing laser light from the source to the positrons and Be+ ions is to use a periscope. For ALPHA-2 this has a path length of 8 m, and therefore requires extensive alignment. If laser cooling were to be introduced to ALPHA-g, a periscope of 15-20 m would be required and the alignment procedure would be highly time intensive. A much easier and less time-consuming method would be to introduce an optical fibre for this purpose. The fibre could be sent through the trap and the only alignment required would be coupling the laser light into the fibre. Optical fibres have the added benefit that a well-collimated, gaussian beam can be produced using a fibre collimator when coupling, which would also reduce the setup time.

As laser cooling in ALPHA requires light in the UV regime, solarisation of the fibre would become an issue. This is a process in which defects on the fibre form due to the high frequency light and cause large losses in transmission [7]. Following the method outlined in Ref. [8], fibres should be hydrogen-loaded and then cured with UV light before use to become solarisation resistant. Using a fibre with a large mode area (LMA) reduces the intensity in the core of the fibre and decreases solarisation there, as well as allowing for easier coupling. However, it is important that single-mode operation remains possible.

Besides solarisation, the dominant issue with optical fibres is that attenuation, the reduction in power due to the light travelling through the fibre, can be very high, with the fibre characterised in this paper demonstrating $\sim$70% loss in transmission in a controlled environment. Bends in the fibre contribute to reduced transmission. Macrobending the fibre can cause the critical angle at the core-cladding interface to be exceeded such that the light is refracted away from the fibre instead of undergoing total internal reflection. Microbends, small scale defects in the fibre core which result from localised stress on the fibre, can cause light to escape as well [9].

It is important to characterise these losses to optimise the working conditions of the fibre. This paper presents a characterisation of the beam profile and bending losses of a hydrogen-loaded and cured, polarisation-maintaining (PM) fibre, and aims to provide direction for future addition of optical fibres to the ALPHA experimental setup.

2 Experimental Setup

The fibre investigated in this paper was a photonic crystal fibre (PCF), LMA-10-PM (NKT Photonics) of length 10 m. Following the method outlined by Colombe *et al.*, the fibre had previously been hydrogen-loaded and cured with UV light to prevent solarization. The fibre had not been stretched in ∼18 months. It was tested using 313 nm light from the Toptica TA-FHG pro laser, a diode laser with two doubling cavities. Input powers between 5 mW and 100 mW were used.

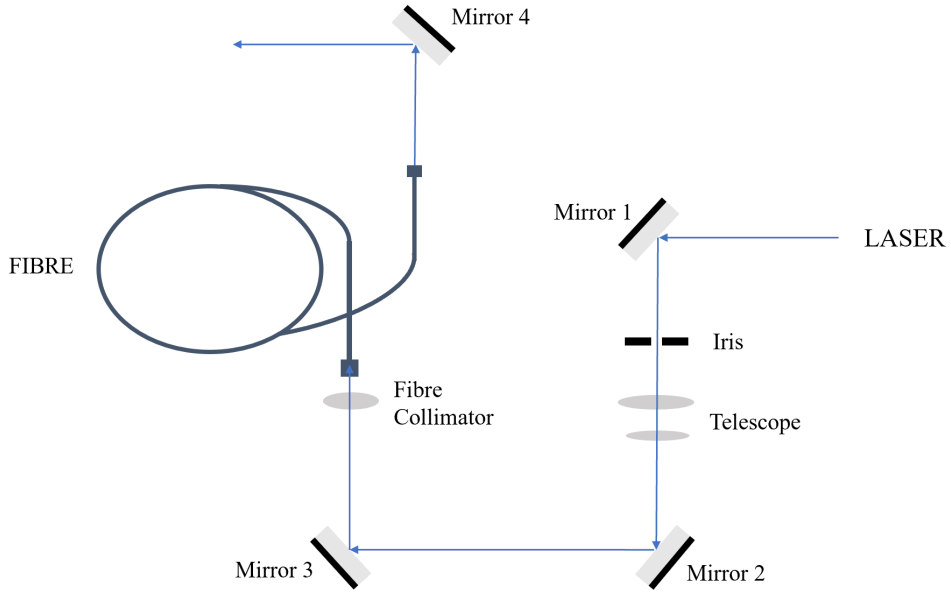

Figure 2: Diagram of the optical table setup

In Fig. 2 the optical table setup is shown. The beam was directed using steering mirrors, and a telescope with lenses of focal lengths 30 cm and 20 cm was used to reduce the beam diameter by a factor of 1.5. The beam was then directed through a half-wave plate before being coupled into the fibre using a fibre collimator and the technique of beam walking.

To measure the input and output powers, a power detector and two different heads were used. A thermal sensor (Coherent, type PM10) was used to measure powers above 10 mW, and an optical sensor (Coherent, type OP-2-UV) was used to measure powers below 10 mW. The transmission was defined as the percentage of output power with respect to the input power. Beam profiling was achieved using a Thorlabs camera beam profiler and the software 'Gaussian Beam', which calculated effective beam diameter, ellipticity (where 100% was perfectly circular), and measured the X and Y profiles.

3 Results and Discussion

3.1 Polarisation Angle

The fibre measured was PM, so finding the optimal polarisation to use was very important. A half-wave plate was installed before the beam was coupled into the fibre to determine the polarisation of light which gave the highest transmission. With an input power of 10 mW, and with the excess fibre length in the coil of diameter 20 cm in which it was stored, a scan of the angle of the half-wave plate vs output power from the fibre was taken. This is shown in Fig. 3. 3 repeats were taken and the average transmission for each angle was calculated. As expected, it was found that the transmission oscillated between 0 and a maximum, with a periodicity of 90°. The highest transmission was found at 45° so this was chosen as

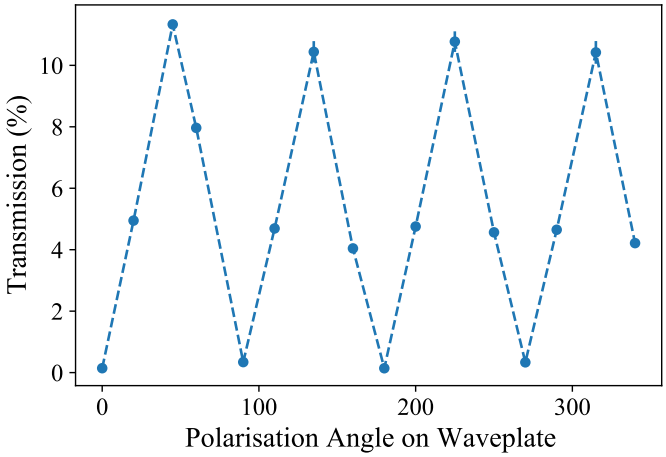

Figure 3: Polarisation angle on the half-wave plate vs the transmission percentage of the fibre.

the position of the half-wave plate for all subsequent measurements.

3.2 Beam Profile

One of the main benefits of using fibres in an optical system is the improved beam profile they produce. Beam profiling measurements taken before and after the fibre was introduced demonstrate this effect.

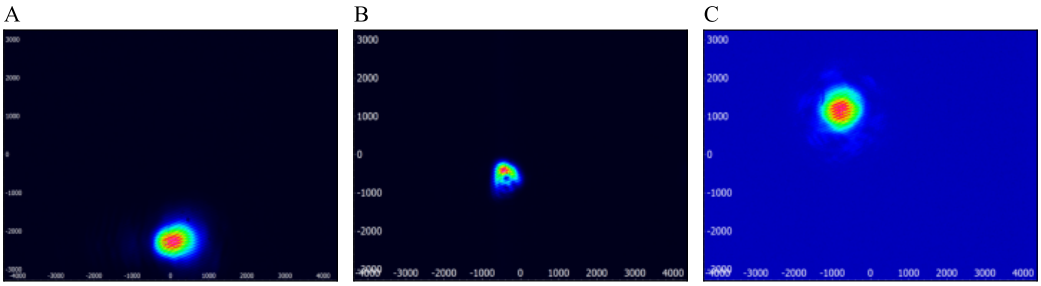

Figure 4: Images of the beam taken with the beam profiler. A was before the telescope, B was after the telescope, C was after the fibre.

Mirror 3 in Fig. 2 was taken as the 0 cm position for beam profiling before the fibre, and all distances were measured relative to this. It is clear that the beam was not perfectly Gaussian at this point. It can be seen in Figs. 4–5 that the Y profile had 2 peaks, and that there was a spot of low intensity on the image of the beam. An iris was introduced before the telescope to remove any side bands of the beam, so this was eliminated as a reason for this beam shape. It can be seen in A of Fig. 4 that the beam before the telescope did not show the same effect, so it is likely that it was a result of a slight misalignment of the beam into the telescope causing light to be sent in unwanted directions and potentially causing some destructive interference. Defects in the lenses may also have caused this.

It can also be seen in Fig. 6 that the effective beam diameter decreased with distance, a sign that the beam was converging. However, by eye the beam seemed to be diverging. It could be possible that the point of low intensity in the beam affected the profiler software's accuracy in determining the effective beam diameter. In future experiments the cause of this beam shape should be investigated more closely so that it can be ensured that the beam is well-collimated before entering the fibre.

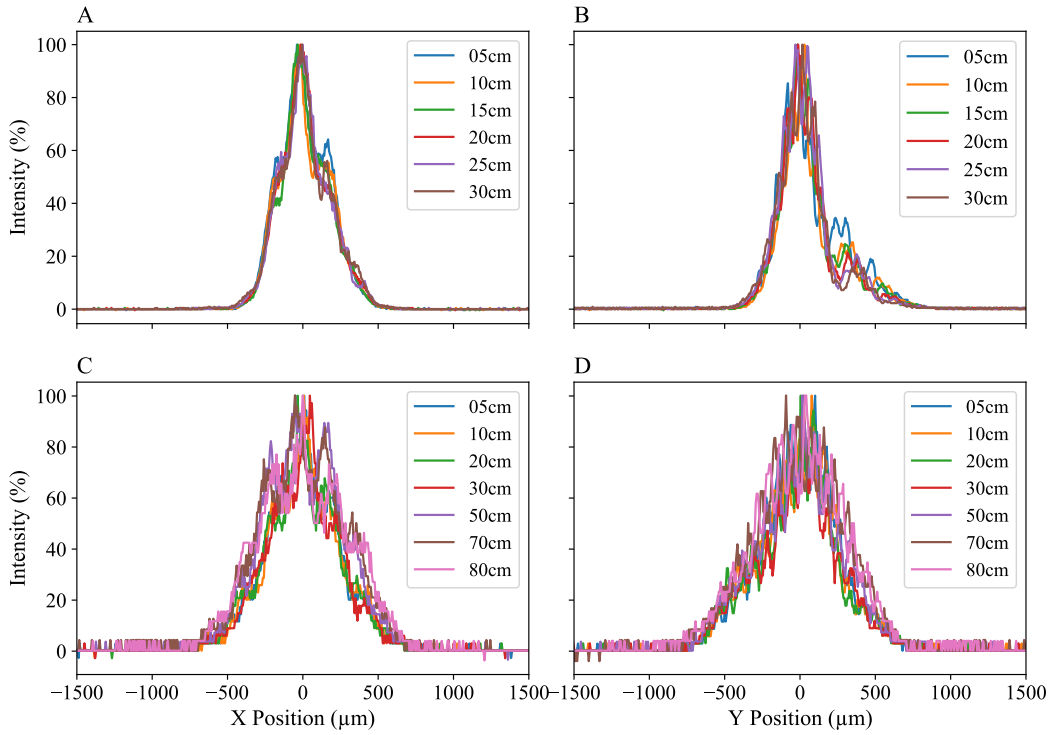

Figure 5: X and Y profiles of the beam at different distances from the source. A and B - beam profile before the fibre. C and D - beam profile after the fibre.

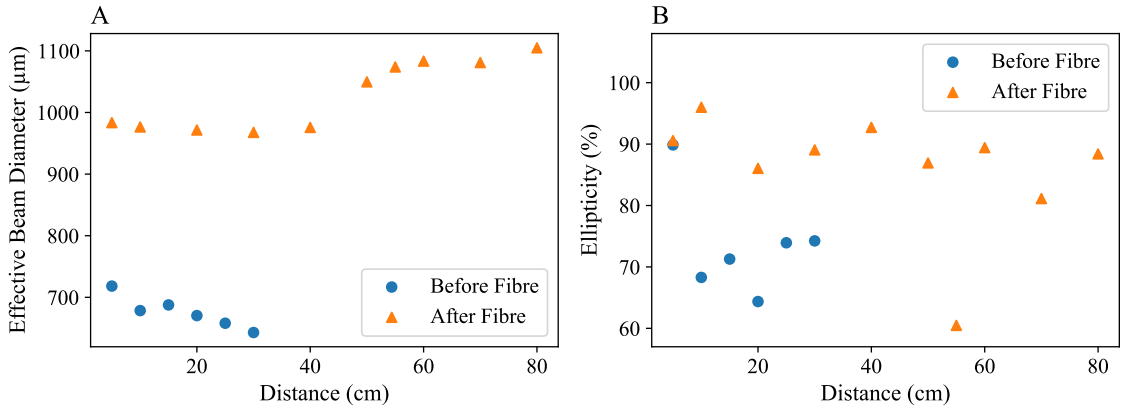

Figure 6: A shows the evolution of the effective beam diameter with distance. B shows the ellipticity of the beam vs distance. Data taken before (blue) and after (orange) the fibre are shown.

Despite the unusual beam shape entering the fibre, post-fibre measurements of the beam profile show that the fibre corrected this effect. Distances were measured relative to the fibre output end. Mirror 4 in Fig. 2 was 35 cm away from the fibre end and used to divert the beam 90° to increase the range of distances the beam could be measured at. The excess fibre length was in a coil of 20 cm diameter. From Figs. 5–6 it can be seen that after the fibre the X and Y profiles were close to Gaussian again and that the beam diverged a little, with the effective beam diameter increasing by about 12% over a distance of 75 cm. However, this increase only became noticeable after the beam was redirected by Mirror 4. It

was noted that the beam was not completely parallel to the optical table, and that it's height above the table increased with distance. Therefore, the slight divergence of the beam could be a feature of it hitting the profiler at different angles for different distances, so different cuts of the beam were measured. The mirror may have amplified this effect which was why it became noticeable from that point onwards. The beam also became more elliptical with distance from the fibre output, this was another sign that the beam was not parallel to the optical table and hitting the beam profiler at an angle.

3.3 Bending Losses

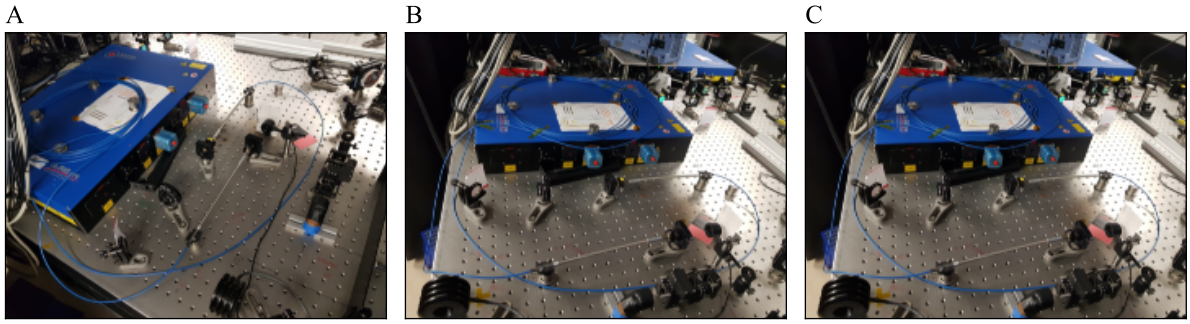

Figure 7: The setup of the excess fibre length for bend diameters investigated. A was 28.5 cm, B was 38 cm, C was 48 cm.

Loss in transmission due to bending of the fibre was measured by introducing loops of various diameters in the excess length of fibre. Loops of diameter 20.0 cm, 28.5 cm, 38.0 cm, and 48.0 cm were investigated by measuring the input power and output power for each. 3 repeats were taken for each data point and averaged before calculating the transmission. The configuration of the fibre for each diameter is shown in Fig. 7. As the fibre had not been stretched it showed some resistance to changing the bend size, and therefore not all loops in each configuration had the exact desired diameter. It is also important to note that the input end of the fibre was very sensitive to any movement, and that changing the bend diameter or height of the fibre close to this end changed the transmission noticeably. For future measurements it would be useful to determine the best position for maximum transmission and then secure the fibre in place.

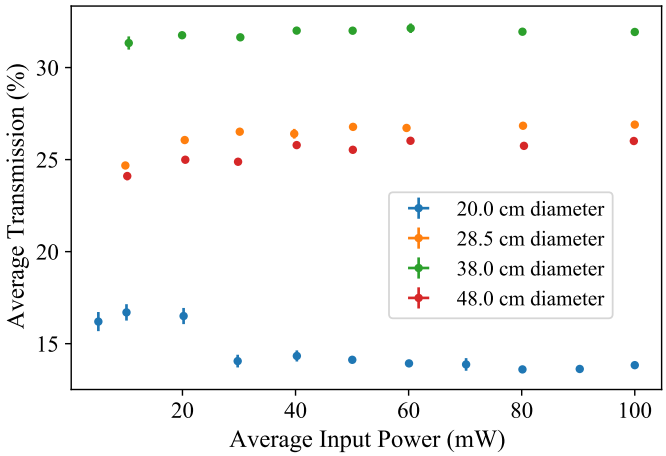

Figure 8: Transmission vs input power for 4 different bend diameters in the fibre.

From Fig. 8 it was determined that a bend diameter of 38.0 cm gave the highest average transmission, reaching (32.1 ± 0.3)% with an average input power of (60.4 ± 0.1) mW. Between 20.0 cm and 38.0 cm the transmission increased as the bend diameter increased. However, the transmission for the 48.0 cm diameter was similar to that of the 28.5 cm diameter, and therefore it was concluded that the transmission peaked around 38.0 cm. Previous work has shown that attenuation increases exponentially as bend diameter decreases [10] [9]. Whilst this trend does not appear to be the case here, more data would be required to determine this, as the sensitivity of the fibre input end to position may have affected the results.

It has also been found that more bends causes higher attenuation [11]. Unfortunately, due to the fibre having a length of 10 m and a lack of space on the optical table it was not possible to investigate the effect bend number had on transmission, or to investigate the bend radius with only one loop in the fibre. This would be an interesting extension to this work, and would likely provide more consistent results as the excess length of fibre could remain in the same straightened position for each loop diameter investigated.

Colombe *et al.* found that for post-cured, hydrogen-loaded fibres, the transmission was independent of input power [ref]. We found that for this fibre the transmission had some dependency on input power: as shown in Fig. 8 transmission increased with input power until 30-50 mW of input power was used, above which the transmission became independent of input power. This effect was seen for all bend diameters used, except 20.0 cm. However, it is believed that the difference seen for this diameter was due to the measurement technique for low input power values, rather than a real trend for small bend diameters. For the first 3 data points for this fibre, 5 mW, 10 mW and 20 mW, the optical sensor was used to measure the input powers, as the lower limit on the range of the thermal sensor was 10 mW. The same optical sensor was used to measure all output powers but the thermal sensor was used to measure input powers $>$20 mW. It was later determined that when using the same input power, the optical sensor consistently measured $\sim$0.97 times that of the thermal sensor. This would explain why the transmission appeared higher for the first 3 data points. However, applying this correction factor did not decrease the transmission enough to match the other data points. There may also have been some error due to moving the optical sensor for each input and output measurement. The position at which the beam hit the sensor caused noticeable variation in the power measured, and it was very unlikely that the same spot was hit for each measurement.

After seeing this effect on the results of the 20.0 cm bend diameter measurement, it was chosen to measure the input powers for all other diameters with the thermal sensor and not use powers below 10 mW. This also allowed us to keep the optical sensor in the same position for all output power measurements to improve consistency.

Previous work has shown that stretching the fibres improves transmission [12]. Therefore further measurements of this fibre should be carried out after stretching it, to determine the highest transmission possible, and to allow for easier manipulation of the excess length of fibre when bending.

3.4 Temperature Effects and Long Term Stability

Temperature has a significant effect on PM optical fibres [13]. This was particularly noticeable in a long-term stability test of this fibre, shown in Fig. 9. The excess length of fibre was in a 28.5 cm diameter loop, as shown in A of Fig. 7. The input power was kept constant at 80 mW and the output power was measured in 1 or 0.5 hour intervals for a period of 5.37 hours. Unfortunately this test was taken when the room temperature was unstable so the true long-term stability was not possible to determine. However, as the room temperature was measured in parallel to the output power, the loss in fibre transmission due to increasing environment temperatures became clear.

From Fig. 9, it can be seen that the transmission with time followed almost an inverse trend to that of room temperature with time. During the measurement period the room temperature increased by

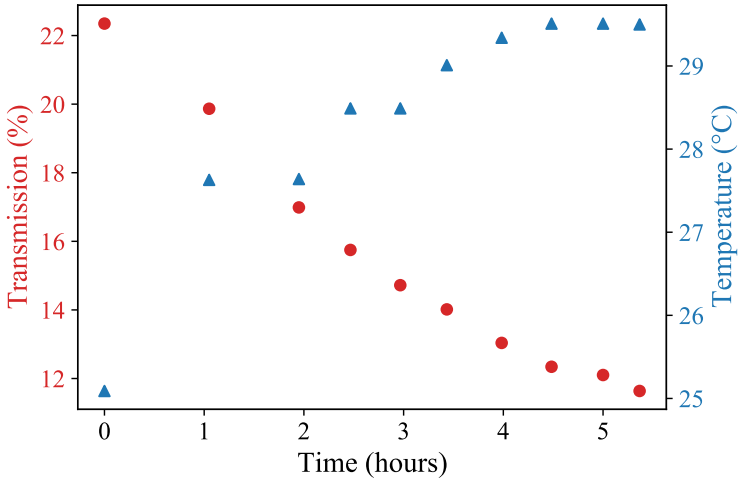

Figure 9: Transmission of fibre with a steady input power of 80 mW (red), and room temperature (blue) measurements over a period of 5.37 hours.

4.4 °C from 25.1 °C to 29.5 °C, and the fibre transmission (normalised to input power) dropped from 22.3% to 11.6%, decreasing by 48%. The input power was also measured at each time and this did not decrease significantly with temperature. Fluctuations in this value were most likely due to the positioning of the power meter sensor, which previously had shown variation dependent on the spot on the surface that the beam hit.

It is clear that higher temperatures reduced the power attenuation of this fibre. PM fibres like the one characterised in this paper have high birefringence, so the refractive index is dependent on the polarisation of the incoming light. Temperature changes can cause transverse thermal expansion of the core and this can affect the birefringence. The thermo-optic effect can also occur, where the refractive index of the crystal changes with temperature. Both of these effects lead to reduced transmission as the chosen polarisation of the light entering the fibre becomes unoptimised [13]. For less temperature dependent results, non-PM fibres should be used in the future. Colombe *et al.* used non-PM fibres and obtained much higher transmissions.

From Fig. 9 it can also be seen that during periods where the room temperature was more constant, especially towards the end of the measurement period, there was still some decrease in transmission with time. In order to confirm the extent to which the fibre loses power with time alone, this long-term stability measurement should be repeated when the room temperature is stable, or after placing the fibre in an insulating box.

4 Conclusions

This paper presented a characterisation of the transmission losses and beam profile correction of an LMA-10-PM optical fibre exposed to 313 nm light.

The maximum transmission through the fibre was (32.1 ± 0.3)%, and this occurred when the fibre had bends of 38 cm diameter and an average input power of 60.4 mW. It was found that the transmission peaked at this bend diameter; diameters lower than 38 cm reduced the transmission of the fibre, however this reduction was also seen for a 48 cm bend diameter. In general, each bend diameter investigated followed the trend that transmission increased with input power up until 30-50 mW, after which it became independent of input power.

Temperature was also a big contributor to transmission losses for this fibre. A long-term measure-

ment of the output power with a constant input power was taken whilst the room temperature increased. The decrease in transmission inversely followed the trend of the temperature increase. In future experiments non-PM fibres should be used to avoid this effect. There were also some data points taken where the temperature remained constant but the transmission continued to decrease. This may suggest that this fibre has some long-term stability issues.

If these losses were minimised through optimising bend diameters in the excess length of fibre and switching to a non-PM fibre, optical fibres could massively reduce time spent on aligning periscopes and provide a simple solution for bringing laser light from the source to the atom trap in the ALPHA-2 OR ALPHA-g experiments.

Acknowledgements

Many thanks to all the team at ALPHA for their support. Particular thanks goes to Maria Beatriz Gomes Goncalves for her guidance and teaching throughout this project.

Bibliography

[1] "How ALPHA Works | ALPHA Experiment, https://alpha.web.cern.ch/how-alpha-works." [Online]. Available: https://alpha.web.cern.ch/how-alpha-works

[2] M. Ahmadi, B. Alves, C. Baker, W. Bertsche, E. Butler, A. Capra, C. Carruth, C. Cesar, M. Charlton, S. Cohen *et al.*, "Antihydrogen accumulation for fundamental symmetry tests," *Nature communications*, vol. 8, no. 1, p. 681, 2017.

[3] J. Danielson and C. Surko, "Torque-balanced high-density steady states of single-component plasmas," *Physical review letters*, vol. 94, no. 3, p. 035001, 2005.

[4] "Stacking | ALPHA Experiment." [Online]. Available: https://alpha.web.cern.ch/science/3-stacking

[5] S. Jonsell and M. Charlton, "On the formation of trappable antihydrogen," *New Journal of Physics*, vol. 20, no. 4, p. 043049, 2018.

[6] C. Baker, W. Bertsche, A. Capra, C. Cesar, M. Charlton, A. C. Mathad, S. Eriksson, A. Evans, N. Evetts, S. Fabbri *et al.*, "Sympathetic cooling of positrons to cryogenic temperatures for antihydrogen production," *Nature communications*, vol. 12, no. 1, p. 6139, 2021.

[7] L. Skuja, H. Hosono, and M. Hirano, "Laser-induced color centers in silica," in *Laser-Induced Damage in Optical Materials: 2000*, vol. 4347. SPIE, 2001, pp. 155–168.

[8] Y. Colombe, D. H. Slichter, A. C. Wilson, D. Leibfried, and D. J. Wineland, "Single-mode optical fiber for high-power, low-loss uv transmission," *Optics express*, vol. 22, no. 16, pp. 19 783–19 793, 2014.

[9] J. A. Jay, "An overview of macrobending and microbending of optical fibers," *White paper of Corning*, pp. 1–21, 2010.

[10] S.-J. Choi, S.-Y. Jeong, C. Lee, K. G. Park, and J.-K. Pan, "Twisted dual-cycle fiber optic bending loss characteristics for strain measurement," *Sensors*, vol. 18, no. 11, p. 4009, 2018.

[11] "Protecting optical networks from micro-bending and macro-bending." [Online]. Available: https://www.acome.com/en/publications/446-expert-opinions/2657-impact-micro-bends-and-macro-bends-optical-budget-telecoms

[12] C. D. Marciniak, H. B. Ball, A. T.-H. Hung, and M. J. Biercuk, "Towards fully commercial, uv-compatible fiber patch cords," *Optics Express*, vol. 25, no. 14, pp. 15 643–15 661, 2017.

[13] P. Ma, N. Song, J. Jin, J. Song, and X. Xu, "Birefringence sensitivity to temperature of polarization maintaining photonic crystal fibers," *Optics & Laser Technology*, vol. 44, no. 6, pp. 1829–1833, 2012.